Volume 11
Number 15
21 April 2020
Pages 3755–4020

Chemical Science

rsc.li/chemical-science

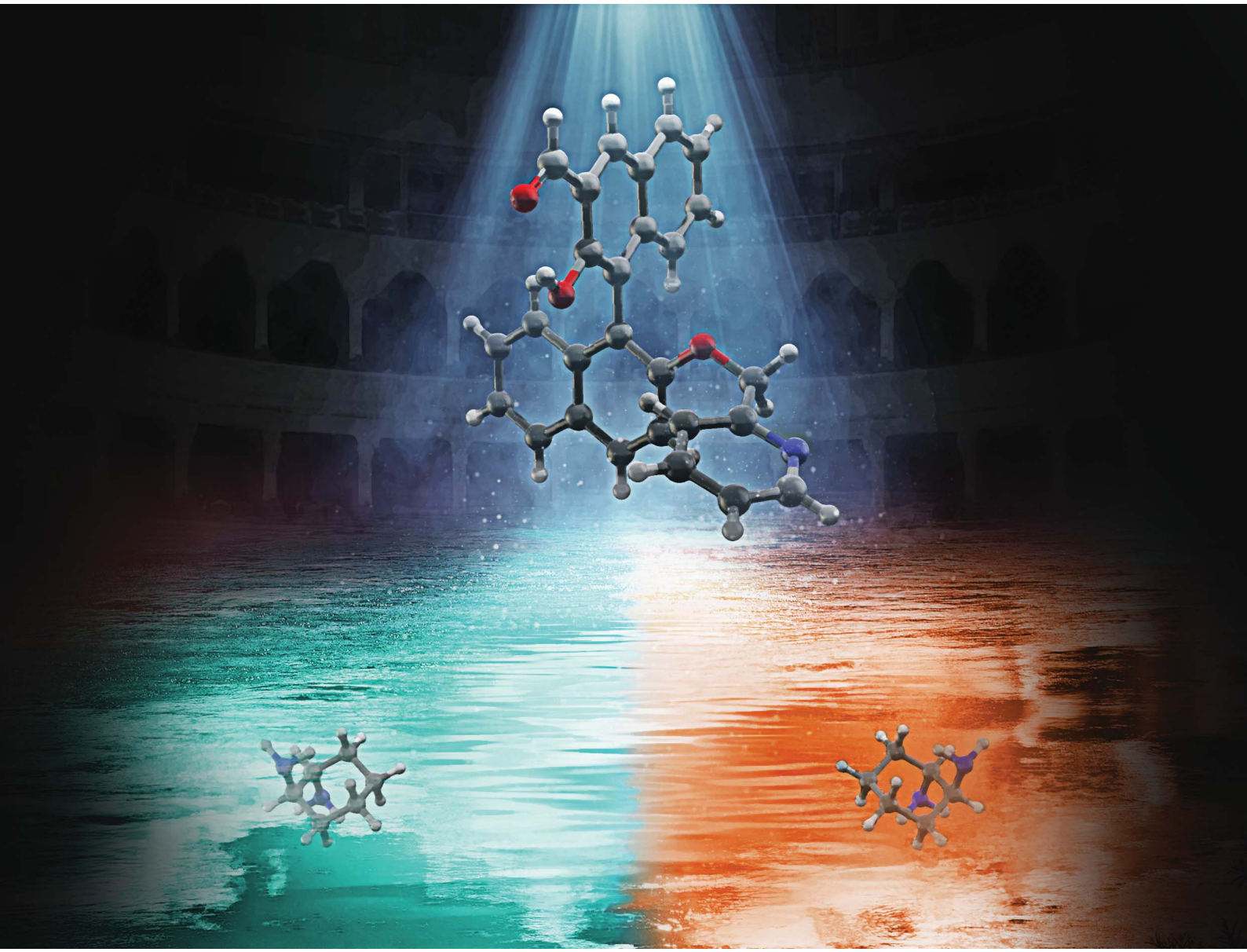

ISSN 2041-6539

ROYAL SOCIETY OF CHEMISTRY

EDGE ARTICLE

Yuji Kubo, Tsuyoshi Minami *et al.*

Accurate chiral pattern recognition for amines from just a single chemosensor

Chemical Science

ROYAL SOCIETY OF CHEMISTRY

EDGE ARTICLE

View Article Online
View Journal | View Issue

Cite this: *Chem. Sci.*, 2020, **11**, 3790

All publication charges for this article have been paid for by the Royal Society of Chemistry

Accurate chiral pattern recognition for amines from just a single chemosensor†

Yui Sasaki, [a] Soya Kojima,[b] Vahid Hamedpour, [a] Riku Kubota, [a] Shin-ya Takizawa, [c] Isao Yoshikawa, [a] Hirohiko Houjou, [a] Yuji Kubo *[b] and Tsuyoshi Minami *[a]

Received 12th January 2020
Accepted 24th February 2020

DOI: 10.1039/d0sc00194e

rsc.li/chemical-science

The current work proposes a novel determination method for enantiomeric excess (ee) in (mono- and di-) amines using molecular self-assembly. A pyridine-attached binaphthyl derivative ((*R*)-**1**) exhibits fluorescence responses based on imine formation between the aldehyde group of (*R*)-**1** and target chiral amines (*i.e.* cyclohexane diamine (**CHDA**), 2-amino-1,2-diphenylethanol (**ADPE**), 1,2-diphenylethylenediamine (**DPDA**), 1-amino-2-indanol (**AID**), and **leucinol**) in the presence of zinc(II) ions (Zn^{2+}). Because of the multi-optical responses which are derived from the variation of chiral complexes, pattern recognition-based discrimination (*i.e.* linear discriminant analysis (LDA)) has been achieved for five types of enantiomeric pairs of amines. Possessing such a discrimination capability in combination with data processing (LDA and an artificial neural network) allows accurate determination (prediction error < 1.8%) of the % ee of individual targets such as **CHDA** which is one of the main components of pharmaceutical drugs. The simple molecular self-assembled system enabled simultaneous multi-chiral discrimination and % ee determination of unknown samples.

Introduction

To date, integration of chemosensors and pattern recognition algorithms has vigorously promoted rapid, accurate and simultaneous sensing of multiple analytes, because finger-print like responses derived from spectral changes in chemosensors can offer valuable information for target discrimination even in complicated environments.[1] To generate finger-print like optical responses in a chemosensor array, diverse chemosensors consisting of many types of backbones,[2] fluorophores[3] and chromophores[4] with several optical detection mechanisms such as intramolecular charge transfer (ICT),[5] photo-induced electron transfer (PeT),[6] and fluorescence resonance energy transfer (FRET)[7] are required. Thus, great efforts are necessary to synthesize and integrate a large amount of chemosensors for obtaining a sufficient number of response patterns in a chemosensor array. However, only a few chemosensors have significantly contributed to the discrimination of analytes in practice.[8] Therefore, a simple array consisting of a very small number of chemosensors enabling the discrimination of a large number of analytes is desired. In addition, the employment of molecular self-assembly can reduce the synthetic effort for chemosensors.[9] Thus, the combination of self-assembled chemosensors and pattern recognition is potentially one of the best methods for chemical sensing.

Chiral compounds are challenging target analytes because of the difficulty in design and synthesis of chiral hosts taking complementarity into account.[10] In this regard, a number of binaphthyl derivatives possessing axial chirality have been synthesized and applied to the chiral recognition.[11] As classical designs of chiral binaphthyl hosts, selective receptors with high structural rigidity have been considerably researched.[12] For example, Pu *et al.* performed chiral discrimination for amino acids based on imine formation of a bisBINOL-based dialdehyde derivative and amino acids.[13] A pyridyl linker moiety of the compound with Zn(II) ions (Zn^{2+}) induced a rigid complex, resulting in an OFF–ON type fluorescence response with chiral selectivity. However, chiral chemosensor arrays for qualitative discrimination of multiple analytes and determination of enantiomeric excess (ee) are still at the frontier.[14] In this regard, Anzenbacher *et al.* reported a self-assembled chemosensor array consisting of three types of binaphthyl-based fluorophores, 2-formylphenylboronic acid and target chiral amines.[15] The proposed array was fabricated by only mixing these components,

[a]*Institute of Industrial Science, The University of Tokyo, 4-6-1 Komaba, Meguro-ku, Tokyo, 153-8505, Japan. E-mail: tminami@iis.u-tokyo.ac.jp; Fax: +81-3-5452-6365; Tel: +81-3-5452-6364*

[b]*Department of Applied Chemistry, Graduate School of Urban Environmental Sciences, Tokyo Metropolitan University, 1-1 Minami-osawa, Hachioji, Tokyo 192-0397, Japan. E-mail: yujik@tmu.ac.jp*

[c]*Department of Basic Science, Graduate School of Arts and Sciences, The University of Tokyo, 3-8-1 Komaba, Meguro-ku, Tokyo, 153-8902, Japan*

† Electronic supplementary information (ESI) available: Fluorescence, UV-Vis and CD titration spectra, quantum yield, emission lifetime, ESI-MS analysis results, experimental details of microarrays, and canonical score plots. CCDC 1976941. For ESI and crystallographic data in CIF or other electronic format see DOI: 10.1039/d0sc00194e

and the array offered chiral discrimination based on an ON–OFF fluorescence response pattern derived from spontaneous iminoboronate formation. In addition, Wolf *et al.* reported biomimicry- and click chemistry-based % ee determination methods for chiral amines using CD spectral changes.[16] Here, we propose chiral pattern recognition using a self-assembled system with a single chiral derivative toward simpler % ee determination.

To perform qualitative and quantitative analyses of chiral targets using a single derivative, various optical response patterns should be generated by multiple self-assembled complexes derived from simple components. Toward this end, we designed a very simple binaphthyl derivative (*R*)-**1** for chiral amine discrimination (Fig. 1). The compound (*R*)-**1** possesses aldehyde and pyridyl groups for spontaneous imine formation with chiral amines in the presence of Zn^{2+}. It is known that the BINOL-derived imine compound has binding selectivity for Zn^{2+} over other transition metal ions.[17,18] In our case, Zn^{2+}-coordination would participate in enantioselective binding behavior toward chiral analytes. Notably, the formation of the rigid imine structure in the presence of Zn^{2+} results in fluorescence enhancement derived from suppressed non-radiative deactivation[19] and intramolecular charge transfer (ICT).[20] The combination of these effects provides OFF–ON fluorescence responses. In contrast, the removal of Zn^{2+} from the **CHDA**-derived complex decreases the fluorescence intensity. Such OFF–ON and ON–OFF responses in the fluorescence intensity and color are the key to determine the % ee with low error by using only a single chemosensor. It is notable that the fluorescence color is analyte amine concentration-dependent; the resultant multi-fluorescence response allows us to develop a simple method for % ee determination in the analyte based on pattern recognition and machine learning. With this intention, we selected cyclohexane diamine (**CHDA**), 2-amino-1,2-diphenylethanol (**ADPE**), 1,2-diphenylethylenediamine (**DPDA**), 1-amino-2-indanol (**AID**), and **leucinol** as targets (Fig. 1) because of their importance in drug development. For example, **CHDA** is present in the backbone of anti-cancer drugs (*e.g.* Eloxatin)[21] and anti-viral drugs (*e.g.* Tamiflu).[22]

Results and discussion

Enantiomeric 3-formyl-2,2′-dihydroxy-1,1′-naphthalene (*R*)-**2** was synthesized according to a method previously reported.[23]

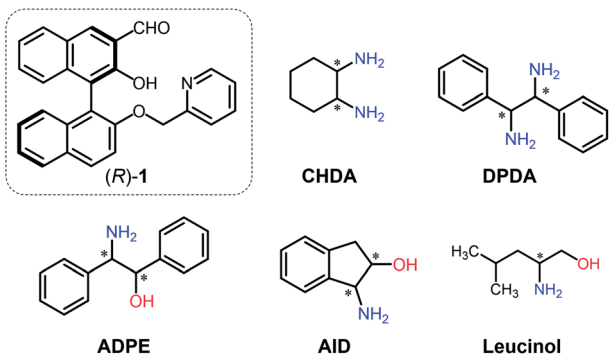

Fig. 1 Chemical structures of (*R*)-**1** and target chiral amines.

The precursor (*R*)-**2** and 2-(chloromethyl)pyridine hydrochloride were mixed; (*R*)-**1** was then obtained by Williamson ether synthesis at 46% yield (Fig. 2). The product (*R*)-**1** was identified by ^{1}H NMR, ^{13}C NMR, fast atom bombardment-mass spectrometry, and elemental analysis (see the ESI†). Moreover, single crystal X-ray diffraction of (*R*)-**1** revealed that the pyridine unit was regioselectively attached (Fig. 2). The binaphthyl unit exhibited an orthogonal structure and the dihedral angle was estimated to be 92° in the solid state (see the ESI for more details†).

Next, we attempted to prepare a self-assembled chiral complex with imine formation between (*R*)-**1** and (1*R*,2*R*)-**CHDA**. (*R*)-**1** and $Zn(OAc)_2$ were first mixed in a 1 : 1 molar ratio, and the mixture was incubated at 25 °C for 1 h. Subsequently, the target amine was injected into the mixture and imine formation proceeded spontaneously under incubation for 24 h. Although we set the incubation time as 24 h, the assay time can be shorter due to the 90% fluorescence response time being within 8 h (Fig. S5† and *vide infra*). The ^{1}H NMR spectra of (*R*)-**1** and the product are shown in Fig. 3. The proton peak assigned to the aldehyde group was observed at 10.30 ppm, while the peak disappeared and a new peak assignable to the imino group was observed at 8.16 ppm after

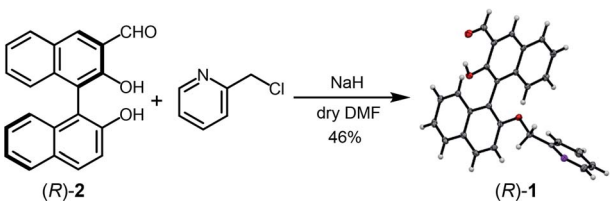

Fig. 2 Synthetic scheme of (*R*)-**1**. The X-ray diffraction structure of (*R*)-**1** is shown at the right side of the scheme. Thermal ellipsoids are scaled to the 50% probability level. The carbon atoms are shown in dark grey, the nitrogen atoms in purple, and the oxygen atoms in red (CCDC 1976941).

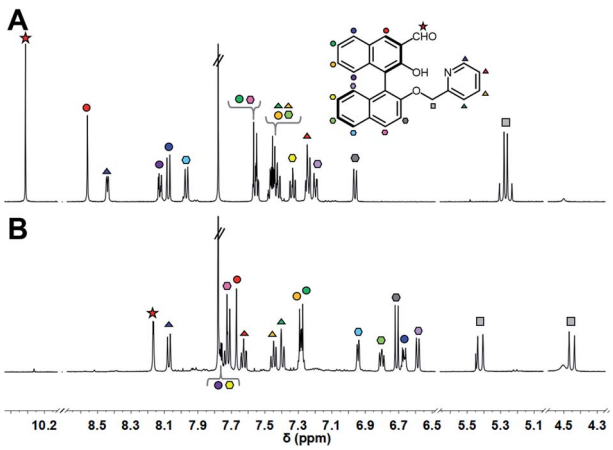

Fig. 3 ^{1}H NMR spectra (500 MHz, $CDCl_3$: MeOD = 1 : 2, *v*/*v*) of (A) (*R*)-**1**, (B) the mixture of (*R*)-**1** and (1*R*,2*R*)-**CHDA** with $Zn(OAc)_2$. [(*R*)-**1**] = 3 mM, [$Zn(OAc)_2$] = 3 mM, [(1*R*,2*R*)-**CHDA**] = 3 mM.

the incubation. Among changes in the chemical shifts of almost all peaks, AB type signals originating from methylene protons were largely split at 5.42 ppm (J = 15.9 Hz) and 4.45 ppm (J = 15.8 Hz), as shown in Fig. 3B. The splitting is most probably due to the high rigidity and asymmetric environment of the product.[19]

To further investigate imine formation, we performed UV-vis, circular dichroism (CD), and fluorescence spectroscopy. The complexation of (*R*)-**1** and **CHDA** by spontaneous imine formation in the presence of $Zn(OAc)_2$ accompanied changes in the multi-step optical properties. As an important result, the fluorescence spectra showed the enantioselectivity of Zn(II)-coordinated (*R*)-**1** for the pair of enantiomers of **CHDA**, with the chiral selectivity ($Int_{(1R,2R)\text{-}CHDA}/Int_{(1S,2S)\text{-}CHDA}$) estimated to be 2500 (Fig. 4A). In this regard, the fluorescence intensity and color showed the difference of complementarity between (1*R*,2*R*)- and (1*S*,2*S*)-**CHDA** for imine formation. Interestingly, the fluorescence pattern of (*R*)-**1** contains OFF–ON and ON–OFF fluorescence signals depending on the concentration of **CHDA** (Fig. 4B). The fluorescence changes were related to UV-vis and CD spectral changes (see the ESI†). The variety of optical response patterns could contribute to the fabrication of pattern-recognition based chemical sensing systems even with a single component.

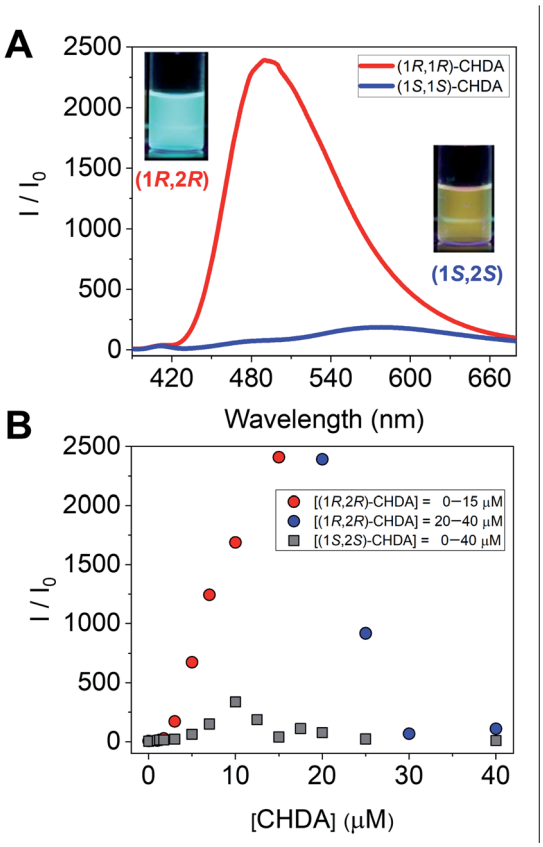

Fig. 4 (A) Fluorescence chiral selectivity of (*R*)-**1** with $Zn(OAc)_2$ for **CHDA** in MeOH. [(*R*)-**1**] = [$Zn(OAc)_2$] = 10 μM, [**CHDA**] = 20 μM, λ_{ex} = 365 nm. Red line: (1*R*,2*R*)-**CHDA** and blue line: (1*S*,2*S*)-**CHDA**. (B) Titration isotherms for **CHDA**. The titration isotherms were obtained by collecting the maximum emission (λ_{em} = 490 nm) intensities at various **CHDA** concentrations.

The complex of (*R*)-**1** (10 μM) and $Zn(OAc)_2$ (10 μM) originally showed no fluorescence, and a fluorescence change was not obtained even after the imine formation process in the low concentration range (0 μM ≤ [(1*R*,2*R*)-**CHDA**] ≤1.7 μM) of (1*R*,2*R*)-**CHDA** (Fig. 5A). Subsequently, the fluorescence enhancement accompanied by a blueshift was observed with the gradual increase of (1*R*,2*R*)-**CHDA** concentrations ([(1*R*,2*R*)-**CHDA**] ≤ 20 μM) (Fig. 5B). The OFF–ON signal in the fluorescence with the blue shift was induced by the increase of the rigidity of the complex and change in the ICT character through the process of Schiff's base formation.[20] Indeed, ^{1}H NMR confirmed that the imine product possessed high rigidity (*vide supra*). Here, a fluorescence ON–OFF signal accompanied by a redshift at an excess amount of (1*R*,2*R*)-**CHDA** was observed (Fig. 5C). The optical change may be induced by decreasing the rigidity of the imine structure; an excess amount of (1*R*,2*R*)-**CHDA** could pull the Zn^{2+} ion out of the imine complex.[24] To reveal whether the optical changes are based on the removal of Zn^{2+} from the **CHDA**-derived complex, we measured the **CHDA**-concentration-dependent ^{1}H NMR spectra of the mixture of (*R*)-**1** and (1*R*,2*R*)-**CHDA** in the presence of $Zn(OAc)_2$. The AB type signals assigned to methylene protons at 5.19 ppm (J = 7.8 Hz) (Fig. S4A†) were largely split up to 1 eq. of (1*R*,2*R*)-**CHDA** at 5.42 ppm (J = 15.9 Hz) and 4.45 ppm (J = 15.8 Hz) (Fig. S4A–D†). On the other hand, the largely split methyl protons disappeared with the addition of an excess amount of (1*R*,2*R*)-**CHDA** (Fig. S4E†). Moreover, in Fig. S4E† signals significantly appeared at 8.55 and 8.35 ppm due to the aromatic protons, the spectral pattern being similar to that of (*R*)-**1** as shown in Fig. S4A.† The proton peak assignable to the aldehyde group was not observed in Fig. S4E,† indicating that a chemical species with an imine structure ((*R*)-**1**–(1*R*,2*R*)-**CHDA**) might be present in the solution. Given that the addition of an excess amount of (1*R*,2*R*)-**CHDA** caused signal broadening in Fig. S4E,† the excess (1*R*,2*R*)-**CHDA** most probably released Zn^{2+} from the Zn^{2+}-coordinated (*R*)-**1**–(1*R*,2*R*)-**CHDA** complex in a competitive binding mode, which confirms that the ON–OFF change in the fluorescence might stem from the removal of Zn^{2+}.

On the other hand, the fluorescence spectra of (*R*)-**1** with $Zn(OAc)_2$ showed a slight blueshift with the addition of (1*S*,2*S*)-**CHDA** (0 μM ≤ [(1*S*,2*S*)-**CHDA**] ≤ 5 μM) (Fig. 5D). Moreover, the fluorescence intensity was gradually enhanced with a blueshift in the spectra ranging from 0.5 to 1.0 eq. of (1*S*,2*S*)-**CHDA** (Fig. 5E). Furthermore, a fluorescence decrease accompanied by a redshift was observed with an excess amount of (1*S*,2*S*)-**CHDA**, the spectral change of which showed a similar tendency to that of (1*R*,2*R*)-**CHDA** (Fig. 5F). Additionally, the emission quantum yields (φ) of each complex were 20% for (1*R*,2*R*)-**CHDA** and 7% for (1*S*,2*S*)-**CHDA**, respectively. Electrospray ionization mass spectrometry (ESI-MS) also indicates multi-complexation such as imine products with or without Zn^{2+}.

Next, we measured the optical properties for imine formation with a monoamine such as **ADPE**. As shown in

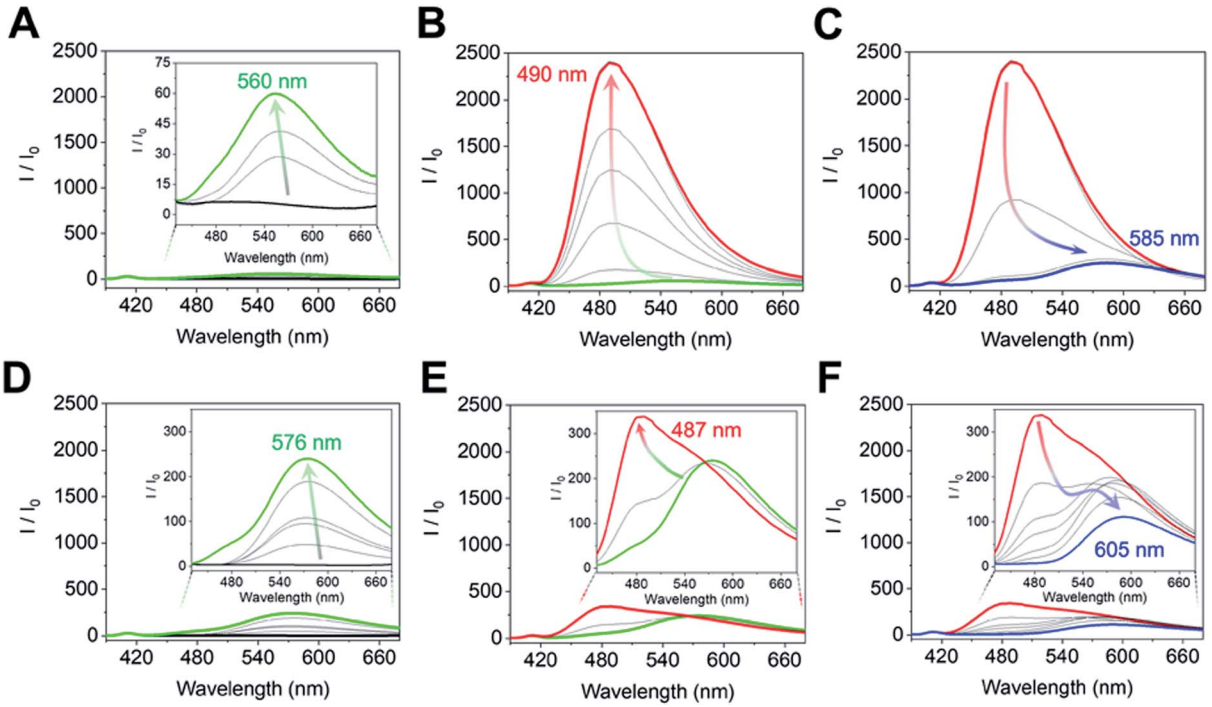

Fig. 5 Fluorescence spectra of (*R*)-**1** with $Zn(OAc)_2$ upon addition of **CHDA** in MeOH at 25 °C. [(*R*)-**1**] = [$Zn(OAc)_2$] = 10 μM, [(1*R*,2*R*)-**CHDA**] = (A) 0–1.7 μM, (B) 1.7–15 μM, and (C) 15–40 μM, [(1*S*,2*S*)-**CHDA**] = (D) 0–5 μM, (E) 5–10 μM, and (F) 10–40 μM. λ_{ex} = 365 nm. The mixture of (*R*)-**1** and (1*R*,2*R*)-**CHDA** with $Zn(OAc)_2$ was incubated at 25 °C for 24 h.

Fig. 6A, the fluorescence intensity was enhanced by the imine formation, and such an optical change was saturated at 1 eq. of (1*S*,2*R*)-**ADPE**. In the case of (1*S*,2*R*)-**ADPE**, removal of the Zn^{2+} ion from the (1*S*,2*R*)-**ADPE** derived complex did not occur unlike in **CHDA**. This is most probably due to the difference in the Lewis acidity between alcohol amine and diamine. In addition, the (1*R*,2*S*)-**ADPE** derived complex showed a relatively weaker OFF–ON fluorescence response than (1*S*,2*R*)-**ADPE**, which could be due to poor complementarity for (*R*)-**1** (Fig. 6B).

Overall, the self-assembled system was able to generate various optical responses to the difference in chirality as well as types of amine derivatives even though only one binaphthyl derivative (*R*)-**1** was used. Hence, the simple system has the potential for simultaneous chiral discrimination and accurate % ee determination for multiple analytes. We set up a fluorescent multi-recognition system based on the proposed simple chiral self-assembly for qualitative and quantitative analysis of five types of enantiomeric pairs of representative amines. For the simultaneous classification of target amines, linear discriminant analysis (LDA)[25] was employed. LDA enables the reduction of the dimensionality of the dataset derived from multi-fluorescence patterns including wavelengths and fluorescence intensities for each target amine and classifies the multivariate data. To evaluate the level of classification accuracy, a leave-one-out cross-validation protocol (*i.e.* the Jackknife method) was used. Moreover, twenty-four repetitions were conducted for each amine in all assays to assess the reproducibility of the fluorescence responses. Student's *t*-test was also applied to exclude four outlier datapoints (of twenty-four repetitions) for decreasing the error. In the LDA results, eleven clusters (control and ten types of chiral amines) were completely discriminated with 100% correct classification (Fig. 7). Remarkably, the classification indicates a difference in the fluorescence responses for chirality, resulting in the grouping of blue (left side) and red clusters (right side). In particular, the distance between (1*R*,2*R*)- and (1*S*,2*S*)-**CHDA** was far more than that between others, since the characteristics of (1*R*,2*R*)- and (1*S*,2*S*)-**CHDA** complexes, such as the fluorescence properties, were completely different from each other. In this assay, we successfully performed the simultaneous discrimination of enantiomers in amines by using a single binaphthyl derivative in the presence of $Zn(OAc)_2$.

In semi-quantitative analysis, simultaneous discrimination of the chirality and concentration of **CHDA** was conducted by using LDA (see the ESI†). The LDA plots show classified clusters of (1*R*,2*R*)-**CHDA** (1 to 30 μM) (circle), (1*S*,2*S*)-**CHDA** (1 to 30 μM) (square), and a control. All tight clusters contain twenty repetitions. 100% correct classification was achieved with chirality and concentration-dependent distances. Indeed, the position of clusters stemmed from the fluorescence responses including the complicated response to **CHDA**. We further attempted % ee discrimination of (1*R*,2*R*)-**CHDA** (0% ee to 100% ee) at 10 μM. As a result of LDA (Fig. 8), all the clusters were discriminated with 100% correct accuracy. Obviously, the position of these clusters showed linearity, meaning that the proposed simple system can determine the % ee. Finally, we

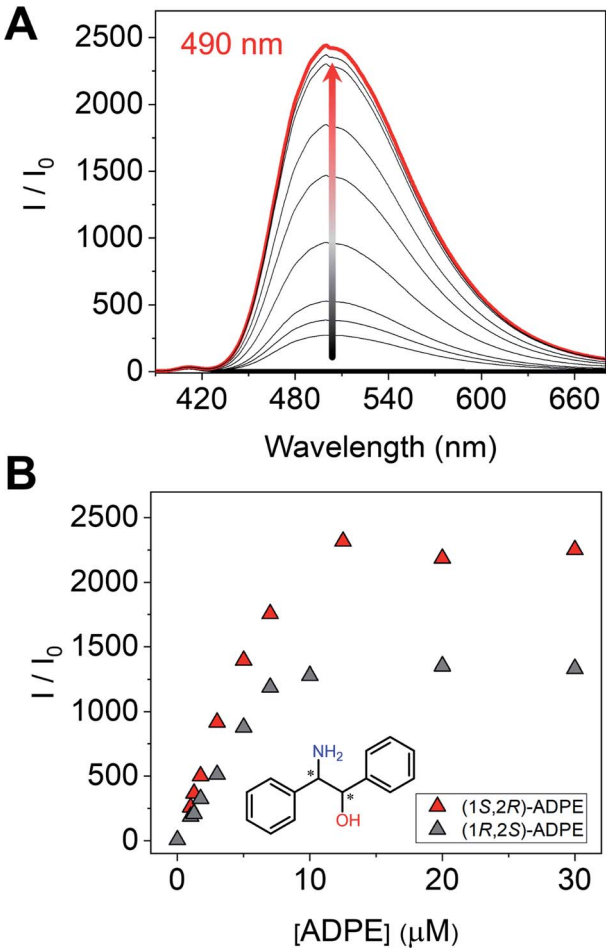

Fig. 6 (A) Fluorescence spectra of (*R*)-**1** with $Zn(OAc)_2$ upon addition of (1*S*,2*R*)-**ADPE** in MeOH at 25 °C. [(*R*)-**1**] = [$Zn(OAc)_2$] = 10 μM, [(1*S*,2*R*)-**ADPE**] = 0–30 μM. λ_{ex} = 365 nm. (B) Titration isotherms for **ADPE**. The titration isotherms were obtained by collecting the maximum emission (λ_{em} = 490 nm) intensities at various **ADPE** concentrations. The mixture of (*R*)-**1** and (1*S*,2*R*)-**ADPE** with $Zn(OAc)_2$ was incubated at 25 °C for 24 h.

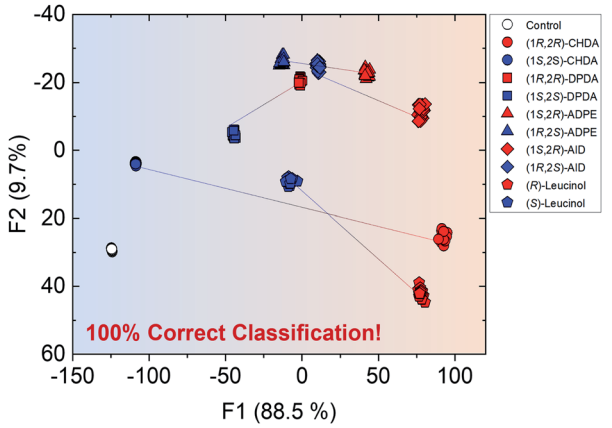

Fig. 7 LDA canonical plots for the qualitative analysis of five types of enantiomeric pairs of amines and a control with 100% correct classification. Twenty repetitions were conducted for each target. [(*R*)-**1**] = [$Zn(OAc)_2$] = [chiral amine] = 10 μM.

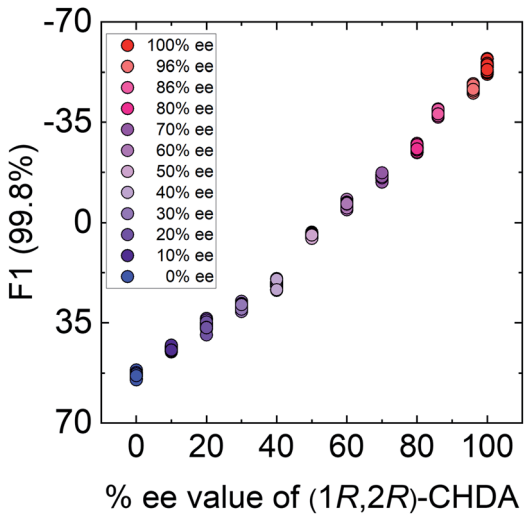

Fig. 8 Results of the semi-quantitative assay based on LDA for the determination of % ee in (1*R*,2*R*)-**CHDA**. Twenty repetitions were conducted for each % ee.

demonstrated the % ee determination of (1*R*,2*R*)-**CHDA** in combination with an artificial neural network (ANN)[26,27] for the prediction of an unknown % ee. In general, for discrimination and/or prediction of target concentrations in complicated mixtures, many types of chemosensors with various characteristics (*e.g.* backbone structures, fluorophores and chromophores) are necessary to prepare cross-reactive response patterns. Given the great efforts in the development of conventional chemosensor arrays, the molecular self-assembly of a single binaphthyl derivative would be a ground-breaking concept toward simple % ee determination. Thus, we decided to predict unknown % ee by using only a single binaphthyl derivative combined with an ANN. The ANN algorithm is one of the most popular multivariate techniques because it can be used for regression, classification and clustering purposes. The ANN mimics the action of a biological network of neurons, and integration with backpropagation (BP)[28] improves the training of feedforward neural networks for supervised learning. Therefore, this ANN-BP was utilized during the regression process. The ANN is a very powerful algorithm to obtain a calibration linear line for targets even though the inset data are complicated because of responses in mixtures or real samples. Hence, the combination of our simple molecular self-assembled system and the ANN model enables highly accurate analysis such as for the determination of the % ee. In this prediction, two types of % ee determination at the (a) large scale (30% ee and 70% ee) and (b) narrow scale (86% ee and 96% ee) were conducted. On the calibration lines, the predicted plots were correctly distributed with low errors (<1.8%) in both the tests (Fig. 9). The multi-detection system composed of a single binaphthyl derivative indicates the possibility of determining the % ee in unknown samples. The results suggest that the proposed model would have the potential for use in practical situations such as drug screening.

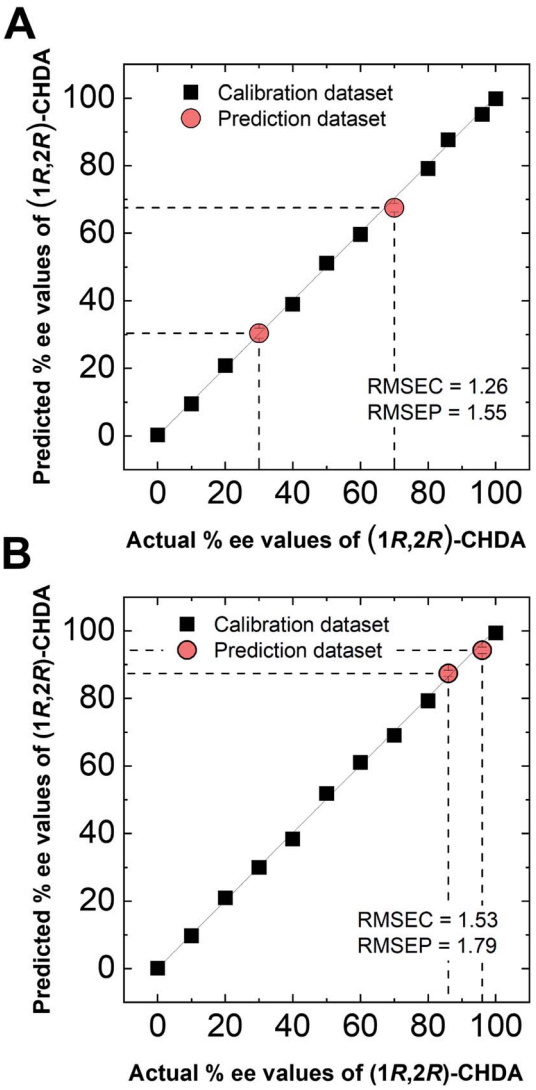

Fig. 9 Results of the artificial neural network (ANN) regression for % ee determination in (1*R*,2*R*)-**CHDA**. The values of the root-mean-square errors of calibration (RMSEC) and prediction (RMSEP) confirm the high accuracy of the built prediction model. The predictions for (A) 30% ee and 70% ee and (B) 86% ee and 96% ee.

Conclusions

We synthesized a novel fluorescent binaphthyl derivative (*R*)-**1** for the determination of % ee in amines based on the imine type molecular self-assembled system. The derivative (*R*)-**1** spontaneously reacted with target amines such as **CHDA**, **ADPE**, **DPDA**, **AID**, and **leucinol** in the presence of $Zn(OAc)_2$, resulting in various optical changes. Remarkably, the proposed chiral imine formation offered many types of complexes based on the difference in analyte structures and concentrations, and the chiral complexes showed multiple optical responses including spectral shifts and intensity changes even with a single binaphthyl derivative. The self-assembled system contributes to discrimination of not only chirality but also similar amine structures including mono- and di-amines. For a high throughput and accurate classification of enantiomers and the number of amines, we demonstrated qualitative analysis of five types of enantiomeric amine pairs by using LDA. The LDA classification results indicate the ability to discriminate a slight difference in structures. Finally, the determination of % ee in the amines was conducted in combination with the ANN for the accurate prediction of unknown % ee. The prediction was successful at both large (30% ee and 70% ee) and narrow (86% ee and 96% ee) scales. Although the prediction was carried out for a single analyte, quantitative % ee determination of mixtures considering amine exchange reactions[29] could be performed using machine learning algorithms.[6b,9f] We successfully performed discrimination of ten types of analytes and prediction of % ee using only one binaphthyl derivative. Thus, we believe that our strategy can open up a new avenue for easy-to-use and accurate chiral pattern recognition from just a single chemosensor.

Conflicts of interest

There are no conflicts to declare.

Acknowledgements

TM thanks the Japan Society for the Promotion of Science (JSPS), Grant-in-Aid for Young Scientists (A), No. 17H04882. YK also thanks the JSPS, Grant-in-Aid for Scientific Research (B), No. 19H02704. YS also thanks the JSPS, Research Fellow for Young Scientists (DC1), No. 18J21190. A part of this work (X-ray single crystallographic analysis) was carried out at the Research Hub for Advanced Nano Characterization, The University of Tokyo.

References

1 For reviews, see: (*a*) K. J. Albert, N. S. Lewis, C. L. Schauer, G. A. Sotzing, S. E. Stitzel, T. P. Vaid and D. R. Walt, *Chem. Rev.*, 2000, **100**, 2595; (*b*) J. J. Lavigne and E. V. Anslyn, *Angew. Chem., Int. Ed.*, 2001, **40**, 3118; (*c*) P. Anzenbacher Jr, P. Lubal, P. Buček, M. A. Palacios and M. E. Kozelkova, *Chem. Soc. Rev.*, 2010, **39**, 3954; (*d*) K. Saha, S. S. Agasti, C. Kim, X. Li and V. M. Rotello, *Chem. Soc. Rev.*, 2012, **112**, 2739; (*e*) Z. Li, J. R. Askim and K. S. Suslick, *Chem. Rev.*, 2019, **119**, 231. For examples, see: (*f*) T. Minami, N. A. Esipenko, A. Akdeniz, B. Zhang, L. Isaacs and P. Anzenbacher Jr, *J. Am. Chem. Soc.*, 2013, **135**, 15238; (*g*) S. Rana, S. G. Elci, R. Mout, A. K. Singla, M. Yazdani, M. Bender, A. Bajaj, K. Saha, U.-H. F. Bunz, F. R. Jirik and V. M. Rotello, *J. Am. Chem. Soc.*, 2016, **138**, 4522; (*h*) Y. Liu, J. Lee, L. Perez, A. D. Gill, R. J. Hooley and W. Zhong, *J. Am. Chem. Soc.*, 2018, **140**, 13869; (*i*) M. A. Beatty, A. J. Selinger, Y. Li and F. Hof, *J. Am. Chem. Soc.*, 2019, **141**, 16763.

2 (*a*) C.-C. You, O. R. Miranda, B. Gider, P. S. Ghosh, I.-B. Kim, B. Erdogan, S. A. Krovi, U. H. F. Bunz and V. M. Rotello, *Nat. Nanotechnol.*, 2007, **2**, 318; (*b*) Z. Wang, M. A. Palacios and P. Anzenbacher Jr, *Anal. Chem.*, 2008, **80**, 7451; (*c*) G. Sener, L. Uzun and A. Denizli, *ACS Appl. Mater. Interfaces*, 2014, **6**, 18395; (*d*) A. M. Mallet, A. B. Davis, D. R. Davis, J. Panella,

K. J. Wallace and M. Bonizzoni, *Chem. Commun.*, 2015, **51**, 16948.

3 (*a*) H. Kwon, W. Jiang and E. T. Kool, *Chem. Sci.*, 2015, **6**, 2575; (*b*) J. Han, B. Wang, M. Bender, K. Seehafer and U. H. F. Bunz, *ACS Appl. Mater. Interfaces*, 2016, **8**, 20415.

4 (*a*) N. A. Rakow and K. S. Suslick, *Nature*, 2000, **406**, 710; (*b*) A. Buryak and K. Severin, *J. Am. Chem. Soc.*, 2005, **127**, 3700; (*c*) K. Chulvi, P. Gaviña, A. M. Costero, S. Gil, M. Parra, R. Gotor, S. Royo, R. Martínez-Máñez, F. Sancenón and J.-L. Vivancos, *Chem. Commun.*, 2012, **48**, 10105.

5 (*a*) J. N. Wilson and U. H. F. Bunz, *J. Am. Chem. Soc.*, 2005, **127**, 4124; (*b*) W. Xu, C. Ren, C. L. Teoh, J. Peng, S. H. Gadre, H.-W. Rhee, C.-L. K. Lee and Y.-T. Chang, *Anal. Chem.*, 2014, **86**, 8763; (*c*) Y.-C. Cai, C. Li and Q.-H. Song, *ACS Sens.*, 2017, **2**, 834.

6 (*a*) M. E. Germain and M. J. Knapp, *J. Am. Chem. Soc.*, 2008, **130**, 5422; (*b*) Y. Sasaki, É. Leclerc, V. Hamedpour, R. Kubota, S. Takizawa, Y. Sakai and T. Minami, *Anal. Chem.*, 2019, **91**, 15570.

7 (*a*) S. Kiyonaka, K. Sada, I. Yoshimura, S. Shinkai, N. Kato and I. Hamachi, *Nat. Mater.*, 2004, **3**, 58; (*b*) Q. Yan, X.-Y. Ding, Z.-H. Chen, S.-F. Xue, X.-Y. Han, Z.-Y. Lin, M. Yang, G. Shi and M. Zhang, *Anal. Chem.*, 2018, **90**, 10536.

8 Y. Liu, T. Minami, R. Nishiyabu, Z. Wang and P. Anzenbacher Jr, *J. Am. Chem. Soc.*, 2013, **135**, 7705.

9 (*a*) B. T. Nguyen and E. V. Anslyn, *Coord. Chem.*, 2006, **250**, 3118. For examples, see; (*b*) Y. Kubo, T. Ishida, A. Kobayashi and T. D. James, *J. Mater. Chem.*, 2005, **15**, 2889; (*c*) H. Miyaji and J. L. Sessler, *Angew. Chem., Int. Ed.*, 2001, **40**, 154; (*d*) P. Metola, E. V. Anslyn, T. D. James and S. D. Bull, *Chem. Sci.*, 2012, **3**, 156; (*e*) Y. Sasaki, T. Minamiki, S. Tokito and T. Minami, *Chem. Commun.*, 2017, **53**, 6561; (*f*) V. Hamedpour, Y. Sasaki, Z. Zhang, R. Kubota and T. Minami, *Anal. Chem.*, 2019, **91**, 13627.

10 For reviews, see: (*a*) X. X. Zhang, J. S. Bradshaw and R. M. Izatt, *Chem. Rev.*, 1997, **97**, 3313; (*b*) C. Moberg, *Angew. Chem., Int. Ed.*, 1998, **37**, 248; (*c*) A. Kumar, S.-S. Sun and A. J. Lees, *Coord. Chem. Rev.*, 2008, **252**, 922; (*d*) H.-J. Schneider and A. K. Yatsimirsky, *Chem. Soc. Rev.*, 2008, **37**, 263; (*e*) K. Staszak, K. Wieszczycka, V. Marturano and B. Tylkowski, *Coord. Chem. Rev.*, 2019, **397**, 76. For examples, see: (*f*) J.-S. Zhao, Y.-B. Ruan, R. Zhou and Y.-B. Jiang, *Chem. Sci.*, 2011, **2**, 937; (*g*) O. Kotova, S. Blasco, B. Twamley, J. O'Brien, R. D. Peacock, J. A. Kitchen, M. Martínez-Calvo and T. Gunnlaugsson, *Chem. Sci.*, 2015, **6**, 457; (*h*) R. Puglisi, F. P. Ballistreri, C. M. A. Gangemi, R. M. Toscano, G. A. Tomaselli, A. Pappalardo and G. T. Sfrazzetto, *New J. Chem.*, 2017, **41**, 911; (*i*) L.-E. Guo, Y. Hong, S.-Y. Zhang, M. Zhang, X.-S. Yan, J.-L. Cao, Z. Li, T. D. James and Y.-B. Jiang, *J. Org. Chem.*, 2018, **83**, 15128.

11 For reviews, see: (*a*) D. J. Cram and J. M. Cram, *Acc. Chem. Res.*, 1978, **11**, 8; (*b*) J. H. Hartley, T. D. James and C. J. Ward, *J. Chem. Soc., Perkin Trans. 1*, 2000, 3155; (*c*) L. Pu, *Acc. Chem. Res.*, 2012, **45**, 150; (*d*) A. Shockravi, A. Javadi and E. Abouzari-Lotf, *RSC Adv.*, 2013, **3**, 6717; (*e*) X. Zhang, J. Yin and J. Yoon, *Chem. Rev.*, 2014, **114**, 4918. For examples, see: (*f*) K. W. Bentley, Y. G. Nam, J. M. Murphy and C. Wolf, *J. Am. Chem. Soc.*, 2013, **135**, 18052; (*g*) Z. Huang, S. Yu, K. Wen, X. Yu and L. Pu, *Chem. Sci.*, 2014, **5**, 3457; (*h*) X. Zhang, C. Wang, P. Wang, J. Du, G. Zhang and L. Pu, *Chem. Sci.*, 2016, **7**, 3614; (*i*) J. Y. C. Lim, I. Marques, V. Félix and P. D. Beer, *Chem. Commun.*, 2018, **54**, 10851; (*j*) X. Xu, L. Qu, J. Song, D. Wu, X. Zhou and H. Xiang, *Chem. Commun.*, 2019, **55**, 9873.

12 (*a*) T. D. James, K. R. A. S. Sandanayake and S. Shinkai, *Nature*, 1995, **374**, 345; (*b*) Y. Kubo, S. Maeda, S. Tokita and M. Kubo, *Nature*, 1996, **382**, 522.

13 Y.-Y. Zhu, X.-D. Wu, S.-X. Gu and L. Pu, *J. Am. Chem. Soc.*, 2019, **141**, 175.

14 (*a*) H. H. Jo, C.-Y. Lin and E. V. Anslyn, *Acc. Chem. Res.*, 2014, **47**, 2212. For examples, see: (*b*) S. Nieto, J. M. Dragna and E. V. Anslyn, *Chem.–Eur. J.*, 2010, **16**, 227; (*c*) S. Yu, W. Plunkett, M. Kim and L. Pu, *J. Am. Chem. Soc.*, 2012, **134**, 20282; (*d*) N. T. Greene and K. D. Shimizu, *J. Am. Chem. Soc.*, 2005, **127**, 5695; (*e*) A. Akdeniz, T. Minami, S. Watanabe, M. Yokoyama, T. Ema and P. Anzenbacher Jr, *Chem. Sci.*, 2016, **7**, 2016; (*f*) F. Y. Thanzeel, A. Sripada and C. Wolf, *J. Am. Chem. Soc.*, 2019, **141**, 16382.

15 E. G. Shcherbakova, T. Minami, V. Brega, T. D. James and P. Anzenbacher Jr, *Angew. Chem., Int. Ed.*, 2015, **54**, 7130.

16 (*a*) S. L. Pilicer, P. R. Bakhshi, K. W. Bentley and C. Wolf, *J. Am. Chem. Soc.*, 2017, **139**, 1758; (*b*) F. Y. Thanzeel and C. Wolf, *Angew. Chem., Int. Ed.*, 2017, **56**, 7276; (*c*) F. Y. Thanzeel, K. Balaraman and C. Wolf, *Nat. Commun.*, 2018, **9**, 5323.

17 S. Wang, G. Men, L. Zhao, Q. Hou and S. Jiang, *Sens. Actuators, B*, 2010, **145**, 826.

18 F. Wang, J. H. Moon, R. Nandhakumar, B. Kang, D. Kim, K. M. Kim, J. Y. Lee and J. Yoon, *Chem. Commun.*, 2013, **49**, 7228.

19 M. E. Shirbhate, R. Nandhakumar, Y. Kim, S.-J. Kim, S. K. Kim and K. M. Kim, *Eur. J. Org. Chem.*, 2018, 4959.

20 K. Komatsu, Y. Urano, H. Kojima and T. Nagano, *J. Am. Chem. Soc.*, 2007, **129**, 13447.

21 D. Höfer, M. Galanski and B. K. Keppler, *Eur. J. Inorg. Chem.*, 2017, 2347.

22 S. Zhu, S. Yu, Y. Wang and D. Ma, *Angew. Chem., Int. Ed.*, 2010, **49**, 4656.

23 Y.-W. Wang, S.-B. Liu, W.-J. Ling and Y. Peng, *Chem. Commun.*, 2016, **52**, 827.

24 M. N. Chaur, D. Collado and J.-M. Lehn, *Chem.–Eur. J.*, 2011, **17**, 248.

25 R. G. Brereton, *Applied Chemometrics for Scientists*, Wiley-VCH, Chichester, 2007.

26 (*a*) A. M. Zain, H. Haron, S. N. Qasem and S. Sharif, *Appl. Math. Model.*, 2012, **36**, 1477; (*b*) M. Jalali-Heravi, M. Arrastia and F. A. Gomez, *Anal. Chem.*, 2015, **87**, 3544.

27 (*a*) S. C. McCleskey, P. N. Floriano, S. L. Wiskur, E. V. Anslyn and J. T. McDevitt, *Tetrahedron*, 2003, **59**, 10089; (*b*) L. Zhu, S. H. Shabbir and E. V. Anslyn, *Chem.–Eur. J.*, 2007, **13**, 99.

28 F. Lussier, V. Thibault, B. Charron, G. Q. Wallace and J.-F. Masson, *Trends Anal. Chem.*, 2020, **7**, 115796.

29 M. Ciaccia and S. Di Stefano, *Org. Biomol. Chem.*, 2015, **13**, 646.

